Separation of Cd and Ni from multicomponent aqueous solutions by nanofiltration and characterization of membrane using IT model

Latesh B. Chaudhari [a,b], Z.V.P. Murthy [a,*]

[a] Department of Chemical Engineering, S.V. National Institute of Technology, Surat 395007, Gujarat, India
[b] Department of Chemical Engineering, N.G. Patel Polytechnic, Isroli-Afwa, Tal. Bardoli, Dist. Surat 394620, Gujarat, India

ARTICLE INFO

ABSTRACT

Removal of heavy metals from wastewater is of critical importance due to their high toxicity and tendency to accumulate in living organisms. In the present work, performance of a nanofiltration (NF) membrane has been studied to separate cadmium and nickel ions from multicomponent aqueous solutions at different operating conditions. It is observed that the separation of cadmium and nickel ions increases with increase in applied pressure and decreases with increase in feed concentration at a constant feed flow rate. The maximum observed solutes rejection of cadmium and nickel ions are 80.57% and 85.27% for $CdCl_2$–$NiCl_2$–water system and 97.26% and 98.90% for $CdSO_4$–$NiSO_4$–water system, respectively, for an initial feed concentration of 0.005 g/L. This difference in rejection is due to the charge density of the anions. It is also observed that the order of solute rejection sequence is inversely proportional to the diffusion coefficient. The NF membrane is characterized by an irreversible thermodynamics (IT) based Spiegler–Kedem model, coupled with film theory. Boundary-layer thickness and membrane transport parameters are estimated using Levenberg–Marquadt method. The estimated parameters are used to predict the membrane performance and found that the predicted values are in satisfactory agreement with the experimental results.

© 2010 Elsevier B.V. All rights reserved.

1. Introduction

Due to the increasingly stringent environmental legislations, treatment of wastewater laden with heavy metals has received considerable attention. Heavy metals are harmful to the environment because of their higher toxicity, non-biodegradable and persistent nature [1]. The pollution sources of these metals in water are industrial activities, such as electroplating, mining, battery manufacturing, metal finishing, textile industries, and automotive industries [2–4]. Different treatment techniques, such as coagulation-flocculation, chemical precipitation, ion exchange and floatation have been tried to treat these wastewaters [5–9]. However, these methods may not be cost effective and contribute to other problems such as slag disposal and extra chemical injection. Due to the high efficiency and convenient operation, membrane filtration operations such as reverse osmosis (RO), complexation-ultrafiltration (UF) and microfiltration (MF) [10–18] have gained popularity in the treatment of wastewater having heavy metals. Compared with RO, nanofiltration (NF) processes have low energy

consumption due to the loose structure of NF membranes. There are several successful studies reported using NF as a tool for the removal of heavy metals like Ni, Cd, Cu, Co, and Pb [19–25]. These results show that NF is a promising technology for the treatment of heavy metals from wastewaters.

In our previous study [25] on $CdCl_2$–$NiSO_4$–water system, it was observed that the overall solute permeability decreases with co-ion valency, while the reflection coefficient increases. Separations on single metal ions from aqueous solutions were reported in the literature, but the same on multicomponent metals is feeble. In the present work, separation of metal ions from multicomponent aqueous solutions ($CdCl_2$–$NiCl_2$–water and $CdSO_4$–$NiSO_4$–water) is performed using a commercial thin-film composite polyamide nanofiltration membrane (Perma-TFC-NF-300, hereafter referred as NF-300 or NF membrane). The performance of the NF membrane and its characterization using the Spiegler–Kedem model, an irreversible thermodynamics model, are reported. The concentration polarization boundary-layer thicknesses, as well as the membrane transport parameters from permeation data are determined.

2. Materials and methods

The NF experiments are performed on a Perma®-pilot scale membrane system (Permionics, Vadodara, India). A rectangular flat

* Corresponding author. Tel.: +91 261 2201641/2223371–2223374; fax: +91 261 2201641/2227334.
 E-mail addresses: zvpm2000@yahoo.com, zvpm@ched.svnit.ac.in (Z.V.P. Murthy).

membrane housing cell is used for the experiments. The details of the setup, characteristics of the NF-300 membrane and experimental procedure are given elsewhere [23–25]. Synthetic samples of wastewater are prepared by adding required amounts of cadmium chloride (CdCl$_2$·2H$_2$O), cadmium sulphate (CdSO$_4$·8H$_2$O), nickel chloride (NiCl$_2$·6H$_2$O) and nickel sulphate (NiSO$_4$·6H$_2$O) to distilled water. All the experiments are performed at a pH of 5.0 ± 0.1, except to study the pH effect on solutes rejection. The NF-300 membrane is characterized by 300 Da cut-off, whose effective membrane surface area is 150 cm^2 (length 15 cm and width 10 cm). For each set of separation data, experiments are performed for 2 h, in batch circulation mode and the permeate samples are collected from high pressure to low pressure for a particular feed concentration and feed flow rate. Both permeate and concentrate are returned to the feed vessel in order to keep constant feed concentration. Samples of permeate are collected at a given time interval to measure the observed salt rejection, R_O ($= 1 - C_{A3}/C_{A1}$); where C_{A1} is the bulk feed solute concentration and C_{A3} is permeate solute concentration; and permeate volume flux (J_V). The metal ion concentrations are measured by an atomic absorption spectrophotometer (SL-173, ELICO Limited, Hyderabad, India) according to standard methods [26]. The setup is rinsed with distilled water for 30 min at 20 atm to clean the system after each set of experiments. This procedure is followed by measurement of pure water permeability (PWP) with distilled water to ensure that the initial membrane PWP is restored. Experiments are carried out for different feed concentrations (0.005–0.25 g/L each of cadmium and nickel salts), feed flow rates (5–15 L/min), applied pressures (4×10^5 to 20×10^5 N/m^2), feed pH (1, 3, 5, 7 and 9) and the corresponding R_O and J_V are measured.

3. Membrane transport model

3.1. Concentration polarization

Transport of solute through NF membranes can be described by irreversible thermodynamics (IT) where the membrane is considered as a black box. In a membrane separation process, the solute concentration near the membrane surface increases when a solute is rejected by the membrane. The build up in the concentration at the membrane–liquid interface is termed as concentration polarization. Gupta et al. [27] developed a novel method to characterize NF and RO membranes that employ the Spiegler–Kedem membrane transport model coupled with the film theory description of the concentration polarization. Attempts have been made to correct the boundary-layer thicknesses determined from literature correlations for the transmembrane flow effects, which are described in the excellent review by Gekas and Hallstrom [28]. According to the film theory, a simple mass balance for the solute in a differential element, using relevant boundary conditions, will give [29]:

$$\left(\frac{C_{A2} - C_{A3}}{C_{A1} - C_{A3}}\right) = \exp\left(\frac{J_V\delta}{D_{AB}}\right) \tag{1}$$

3.2. Modified irreversible thermodynamics model

As mentioned earlier, transport of a solute through NF membranes can be described by an IT model, named the Spiegler–Kedem model [30–33]. Spiegler and Kedem [30] proposed relations for permeate volume flux and solute flux through a membrane to obtain the following relations:

$$J_V = L_P(\Delta P - \sigma\,\Delta\pi) \tag{2}$$

$$R = \sigma\frac{(1-F)}{(1-\sigma F)} \tag{3}$$

$$F = \exp\left(-\frac{(1-\sigma)}{P_M}J_V\right) \tag{4}$$

The Spiegler–Kedem model was used widely to interpret/predict the performance of RO/NF/UF membranes [34–38]. The $\Delta\pi$ is given by the van't Hoff equation [27]:

$$\Delta\pi = \phi\nu(C_{A2} - C_{A3})R_gT \tag{5}$$

The values of osmotic coefficients of the salts studied here are taken from the literature [39–41]. It is important to note that, due to the concentration polarization, the salt solution at the membrane surface cannot be assumed to be dilute. The values of osmotic coefficients used in this study are 0.534, 0.8907, 0.388 and 0.584 for cadmium chloride, nickel chloride, cadmium sulphate and nickel sulphate salts, respectively. Substituting $\Delta\pi$ from Eq. (5) into Eq. (2) will give:

$$J_V = L_p[\Delta P - \sigma\phi\nu(C_{A2} - C_{A3})R_gT] \tag{6}$$

The J_V and R_O cannot be directly used to analyze the permeation data since they contain boundary-layer concentration (C_{A2}) that cannot be measured directly. Combining the Eqs. (6) and (1) will eliminate the term ($C_{A2} - C_{A3}$) and the resulting equation for the permeate flux can be written as [27]:

$$\Delta P = \frac{J_V}{L_p} + \sigma\phi\nu(C_{A1} - C_{A3})R_gT\,\exp\left(\frac{J_V}{D_{AB}/\delta}\right) \tag{7}$$

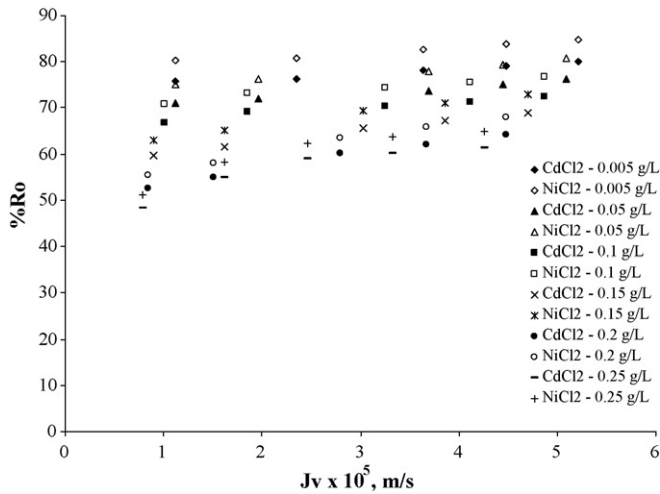Eq. (7) is the combined membrane transport and concentration polarization model used in the study.

Fig. 1. Influence of permeate volume flux on the observed solute rejection of CdCl$_2$–NiCl$_2$–water system at different feed concentrations and feed flow rate of 10 L/min.

4. Results and discussion

4.1. Effect of applied pressure, type of anion and feed concentration

Rejection of cadmium and nickel ions from CdCl$_2$–NiCl$_2$–water and CdSO$_4$–NiSO$_4$–water systems is plotted against the permeate volume flux at different feed concentrations (see Figs. 1 and 2). As shown in Figs. 1 and 2, rejection of cadmium and nickel ions increases slightly with increase in permeate volume flux for different feed concentrations (0.005–0.25 g/L), with the applied pressure ranging between 4×10^5 and 20×10^5 N/m^2. The maximum observed rejections of cadmium and nickel ions are found to be 80.57% and 85.27% for CdCl$_2$–NiCl$_2$–water system and 97.26% and 98.90% for CdSO$_4$–NiSO$_4$–water system, respectively, for an initial feed concentration of 0.005 g/L, applied pressure 20×10^5 N/m^2 and feed flow rate of 15 L/min. It can be seen from Figs. 1 and 2 that the rejections of cadmium and nickel ions from CdSO$_4$–NiSO$_4$–water system are higher than the CdCl$_2$–NiCl$_2$–water system, which is typical phenomena of NF membrane [32,42]. Rejection efficiency increases with increase in valency of the anion due to the increased electrostatic repulsion by
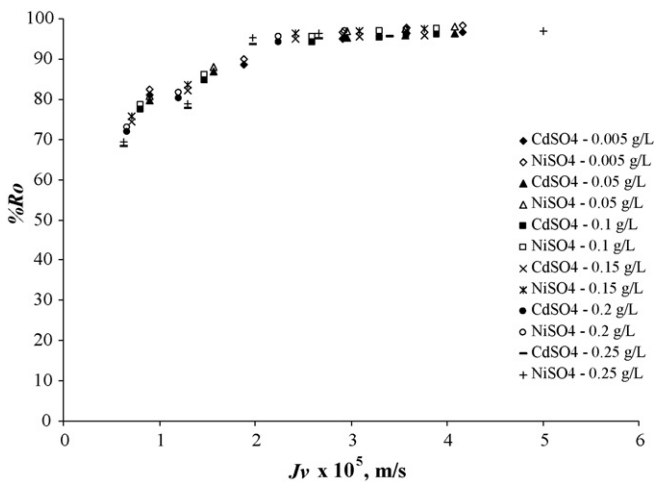

Fig. 2. Influence of permeate volume flux on the observed solute rejection of CdSO$_4$–NiSO$_4$–water system at different feed concentrations and feed flow rate of 10 L/min.
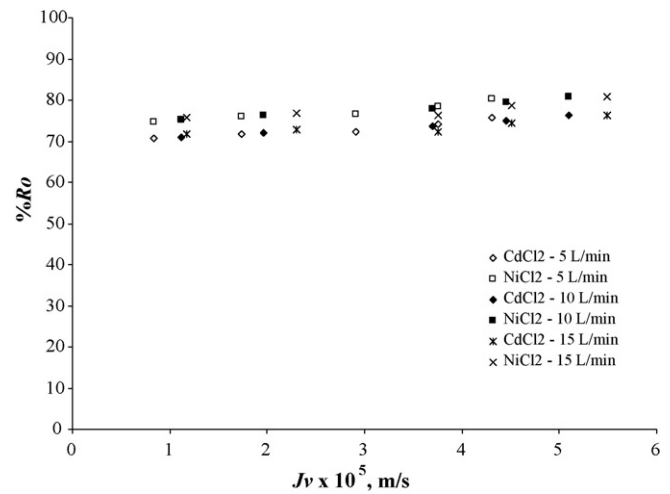

Fig. 3. Influence of permeate volume flux on the observed solute rejection of CdCl$_2$–NiCl$_2$–water system at different feed flow rates and feed concentration of 50 ppm.

the membrane, which is a characteristic property of NF membranes. In our previous work [25], we have reported that the NF membrane showed the following rejection sequence: $R_O(\text{Ni}^{2+}) > R_O(\text{Cd}^{2+})$ for NiSO$_4$–CdCl$_2$–water system. It can be interpreted from this result that the rejection was higher for cation (Ni^{2+}) associated with sulphate than cation (Cd^{2+}) associated with monovalent anion (Cl$^-$). The chloride ions are less hydrated than the sulphate ions (1047 and 325 kJ mol/L for chloride and sulphate, respectively) resulting in less rejection of chloride ions [31,32,43]. For the same valency anions, rejection sequence can be found by comparing the diffusion coefficients of the cadmium and nickel ions. The diffusion coefficients of nickel and cadmium in water at 25 °C are 1.32×10^{-5} and 1.44×10^{-5} cm^2/s [44]. The order of diffusion coefficients is inversely reflected in the rejection sequence; hence the diffusion seems to be an important factor in the transport mechanism. As the diffusion coefficient of cadmium is higher than that of nickel, a high diffusion contribution can be expected, resulting in a lower rejection, which is in line with the reported trends [19,42,45].

4.2. Effect of cross-flow velocity

Figs. 3 and 4 show the effect of cross-flow velocity from 0.0055 to 0.017 m/s (or 5–15 L/min) on the rejection of cadmium and nickel ions with change in applied pressure. The percentage rejection of solute increases on increasing the cross-flow velocity at the same operating pressure. The main purpose of increasing the cross-flow velocity is to increase the mass transfer coefficient, D_{AB}/δ, which in turn increases the solute rejection. Similar results were found for the nickel ions by Ahn et al. [21] and for the zinc ions by Frares et al. [46].

4.3. Effect of pH

Fig. 5 shows the rejection of ions at various pH values. The pH is adjusted by the addition of HCl and NaOH, depending upon the need. The concentration, pressure and flow rate are fixed at 0.05 g/L, 8×10^5 N/m^2 and 15 L/min, respectively. It can be seen from Fig. 5 that for CdSO$_4$–NiSO$_4$–water system there is no significant change of rejection of cadmium and nickel ions with pH. Similar results were observed for nickel ions by Ahn et al. [21]. For CdCl$_2$–NiCl$_2$–water system, rejections are dependent on pH. The rejection is sensitive to pH change, where R_O reached high at pH 1, then decreased to minimum at pH 5 and then increased again.
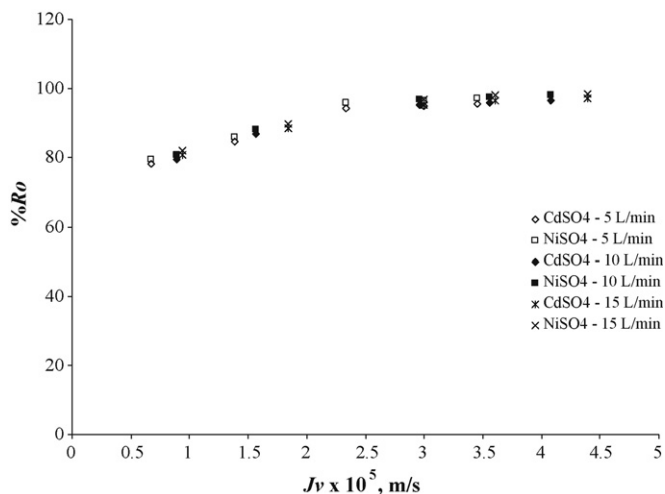
Fig. 4. Influence of permeate volume flux on the observed solute rejection of CdSO$_4$–NiSO$_4$–water system at different feed flow rates and feed concentration of 50 ppm.
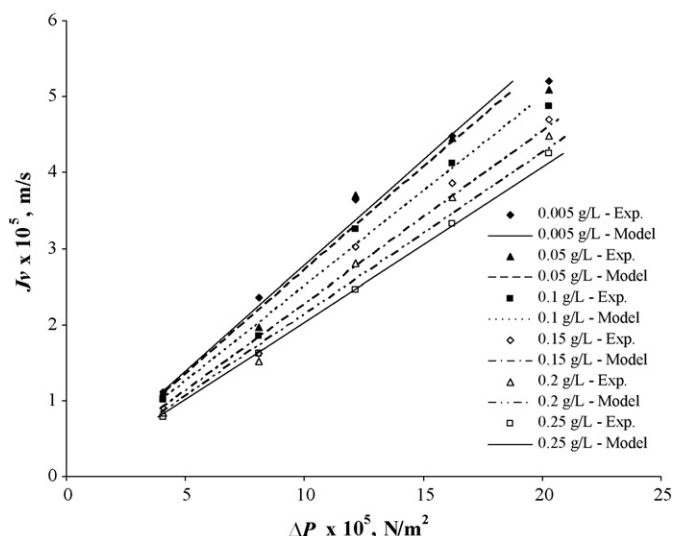

Fig. 6. Results from combined membrane transport and concentration polarization model for CdCl$_2$–NiCl$_2$–water system by using NF-300 membrane at different feed concentrations and feed flow rate of 10 L/min.

Fig. 5. Influence of pH on the observed solute rejection for CdCl$_2$–NiCl$_2$–water and CdSO$_4$–NiSO$_4$–water system (feed concentration = 50 ppm, applied pressure = 8 × 10^5 N/m^2, feed flow rate = 10 L/min).

Fig. 7. Results from combined membrane transport and concentration polarization model for CdSO$_4$–NiSO$_4$–water system by using NF-300 membrane at different feed concentrations and feed flow rate of 10 L/min.
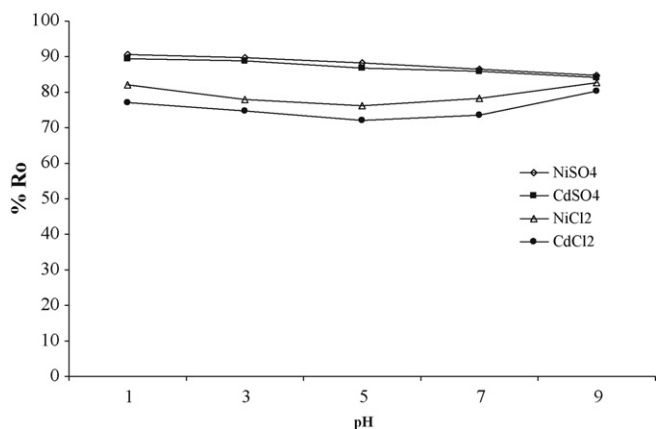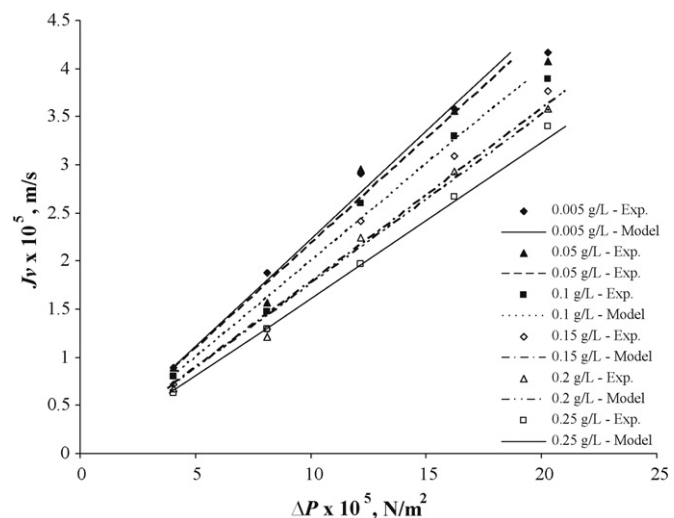
Table 1
Summary of the calculated values of L_P and D_{AB}/δ at various operating conditions for the binary salt system (PWP = 3.64 × 10^{-11} m^3/s N).

| Set	Feed rate (L/min)	Feed conc. (ppm)	$L_{P,Caculated}$ (×10^{11} m^3/s N)				D_{AB}/δ (×10^5 m/s)				σ			
			CdSO$_4$	NiSO$_4$	CdCl$_2$	NiCl$_2$	CdSO$_4$	NiSO$_4$	CdCl$_2$	NiCl$_2$	CdSO$_4$	NiSO$_4$	CdCl$_2$	NiCl$_2$
1	5	5	1.86	1.85	2.33	2.29	8.73	8.66	8.65	8.61	0.9873	0.9958	0.9032	0.9218
2	10	5	2.23	2.22	2.78	2.70	8.93	8.85	8.88	8.83	0.9868	0.9955	0.8976	0.9162
3	15	5	2.33	2.44	3.13	3.03	9.13	9.05	9.08	9.03	0.9863	0.9951	0.8861	0.9051
4	5	50	1.79	1.79	2.22	2.17	8.55	8.47	8.50	8.45	0.9852	0.9944	0.8753	0.8939
5	10	50	2.33	2.33	2.71	2.64	8.77	8.70	8.73	8.67	0.9847	0.9941	0.8660	0.8846
6	15	50	2.34	2.33	2.95	2.87	8.93	8.85	8.88	8.83	0.9842	0.9938	0.8567	0.8753
7	5	100	1.70	1.69	2.13	2.08	8.38	8.31	8.33	8.28	0.9832	0.9931	0.8493	0.8679
8	10	100	2.00	2.00	2.50	2.44	8.56	8.48	8.51	8.47	0.9827	0.9927	0.8348	0.8534
9	15	100	2.18	2.17	2.78	2.70	8.94	8.33	8.73	8.68	0.9822	0.9924	0.8233	0.8419
10	5	150	1.49	1.49	1.89	1.85	8.40	8.14	8.17	7.52	0.9811	0.9921	0.8159	0.8344
11	10	150	1.79	1.79	2.27	2.22	8.47	8.31	8.33	8.29	0.9806	0.9917	0.8084	0.8270
12	15	150	2.09	2.08	2.63	2.56	8.56	8.49	8.52	8.48	0.9801	0.9914	0.7921	0.8106
13	5	200	1.43	1.43	1.79	1.75	8.75	7.98	8.01	7.96	0.9791	0.9904	0.7861	0.8047
14	10	200	1.76	1.76	2.13	2.08	8.92	8.12	8.15	7.50	0.9786	0.9900	0.7750	0.7935
15	15	200	1.93	1.93	2.50	2.44	9.09	8.31	8.34	8.29	0.9781	0.9897	0.7620	0.7805
16	5	250	1.37	1.37	1.72	1.69	8.56	7.82	7.84	7.81	0.9771	0.9890	0.7545	0.7731
17	10	250	1.62	1.62	2.04	2.00	8.73	7.96	7.99	7.95	0.9765	0.9887	0.7415	0.7601
18	15	250	1.79	1.79	2.27	2.22	8.91	8.12	8.14	8.11	0.9760	0.9883	0.7177	0.7363
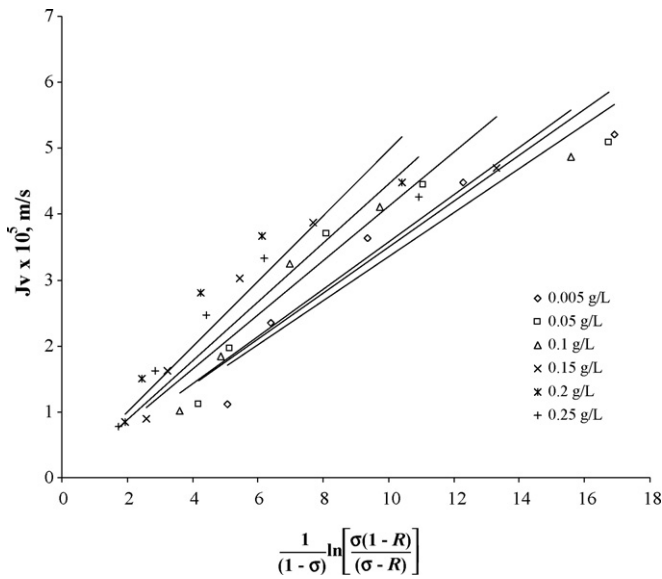
Fig. 8. Plot of permeate volume flux as a function of R for the cadmium ions ($CdCl_2$–$NiCl_2$–water system) to determine P_M (feed flow rate = 10 L/min).
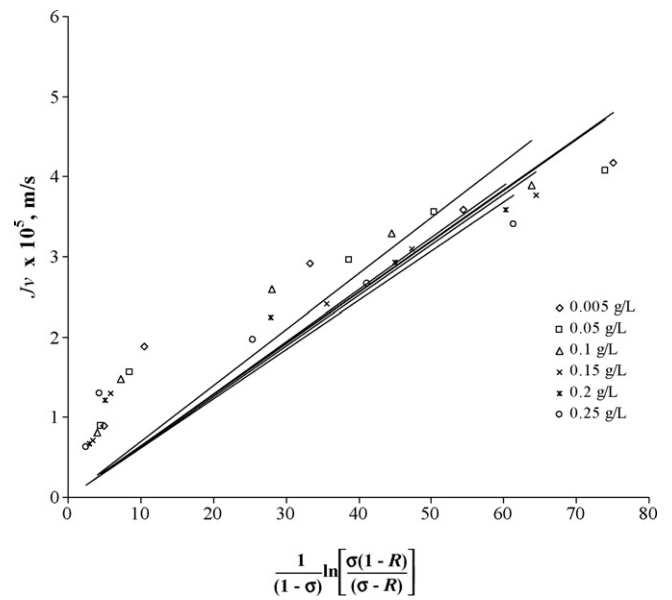
In the present case, it may be said that at pH 5 the membrane iso-electric point (IEP) is approached. Similar IEP for cadmium ions was observed by Garba et al. [20] and Ballet et al. [31].

4.4. Determination of membrane transport parameters

The Levenberg–Marquardt method [47], a non-linear parameter estimation method, is used to estimate the parameters; namely hydraulic permeability coefficient (L_p), reflection coefficient (σ) and D_{AB}/δ. The data supplied are ΔP and J_V taken at different operating pressures keeping feed flow rate and feed solute concentration constant for each set of data. The parameters L_p, σ, and D_{AB}/δ estimated from Eq. (7) are shown in Table 1. It can be observed from Table 1 that with increase in feed flow rate, from 5 to 15 L/min, the value of D_{AB}/δ is increasing at same feed concentration; that means the concentration polarization boundary-layer thickness directly affected by the flow rate in cross-flow mode. Thus, one way of minimizing concentration polarization, to some extent, is to reduce the boundary-layer thickness by increasing shear force at the membrane surface with high feed flow rates [48]. It can be seen from

Fig. 9. Plot of permeate volume flux as a function of R for the cadmium ions ($CdSO_4$–$NiSO_4$–water system) to determine P_M (feed flow rate = 10 L/min).

Table 1 that the σ decreases with increase in feed solute concentration. It is found that the σ for each salt increases with co-ion valency. These parameters are then used to calculate the applied pressure for different values of J_V. It can be seen from Figs. 6 and 7 that the model predictions for the pressure values are in satisfactory agreement with the experimental results. The difference between experimental and model results increases when the pressure increases at lower concentration. It can be concluded that the model is valid for a wide range of concentration (from 0.005 to 0.25 g/L) for binary salts. It can also be seen from Figs. 6 and 7 that with increasing concentration from 0.005 to 0.25 g/L the permeate volume flux decreases.

Eq. (3) can be rearranged by putting the value of F to get [27]:

$$J_V = \frac{P_M}{(1-\sigma)} \ln \left[\frac{\sigma(1-R)}{(\sigma-R)} \right] \tag{8}$$

In case of binary salt ($CdCl_2$–$NiCl_2$–water and $CdSO_4$–$NiSO_4$–water) systems, the P_M can be obtained from the slope of plot of J_V vs. the coefficient of P_M on the right-hand-

Table 2
Summary of the membrane transport parameters at various operating conditions for binary salt system.

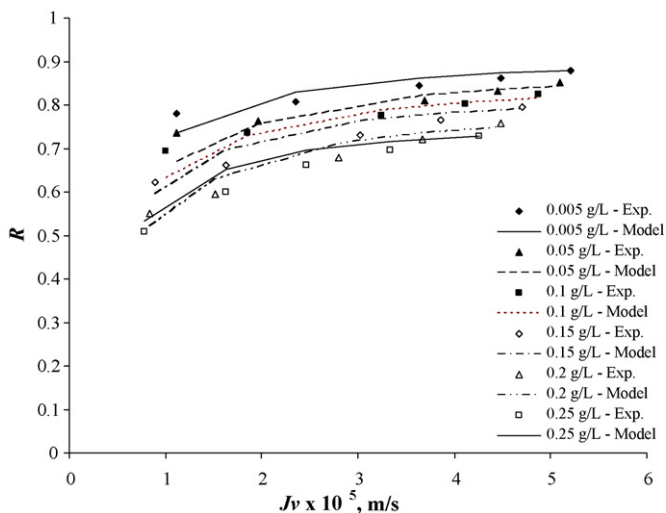| Set	Feed rate (L/min)	Feed conc. (ppm)	Solute permeability P_M ($\times 10^7$ m/s)			
			$CdSO_4$	$NiSO_4$	$CdCl_2$	$NiCl_2$
1	5	5	8	6	40	30
2	10	5	6	4	30	20
3	15	5	5	3	30	20
4	5	50	8	6	40	30
5	10	50	6	5	40	20
6	15	50	6	3	40	30
7	5	100	8	6	30	30
8	10	100	7	5	40	30
9	15	100	4	2	40	20
10	5	150	8	6	50	40
11	10	150	6	5	40	20
12	15	150	3	3	40	20
13	5	200	8	6	60	50
14	10	200	6	5	50	50
15	15	200	3	3	50	40
16	5	250	7	6	60	50
17	10	250	6	5	40	20
18	15	250	2	2	40	40

Fig. 10. Plot of true rejection (R) vs. permeate flux (J_V) and its comparison with the values calculated using irreversible thermodynamics model for the $CdCl_2$–$NiCl_2$–water system at different feed concentrations and feed flow rate of 10 L/min.

side of Eq. (8); by non-linear curve fitting method. These plots are shown in Figs. 8 and 9 for the cadmium and nickel ions, using $CdCl_2$–$NiCl_2$–water and $CdSO_4$–$NiSO_4$–water systems, respectively, at different feed concentrations (0.005–0.25 g/L) and a feed flow rate of 10 L/min. The membrane parameters estimated by this method are summarized in Table 2 and the percent error is in the range of 0.5–6.7. It can be seen from Table 2 that the P_M decreases with co-ion valency. The value of P_M is highly dependent on the type of anion of the electrolyte solute. Strongly solvated anions ($SO_4{}^{2-}$) lead to lower values of P_M in comparison with the less solvated anions (Cl^-). Similar trends are reported in literature for different monovalent and divalent salts by several researchers [20,21,25,31,32].

The plots of true solutes rejection (R) vs. J_V are shown in Figs. 10 and 11 for $CdCl_2$–$NiCl_2$–water and $CdSO_4$–$NiSO_4$–water systems, respectively. It can be seen from Figs. 10 and 11 that the R calculated at various operating conditions increases with
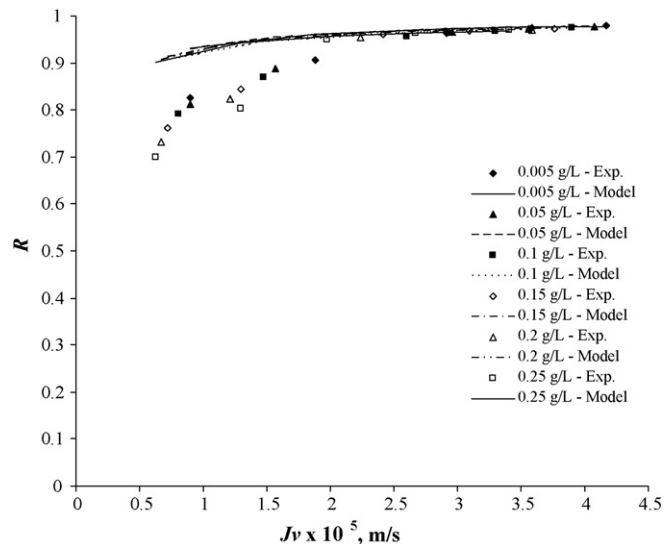

Fig. 11. Plot of true rejection (R) vs. permeate volume flux (J_V) and its comparison with the values calculated using irreversible thermodynamics model for the $CdSO_4$–$NiSO_4$–water system at different feed concentrations and feed flow rate of 10 L/min.

increasing applied pressure. This unique correlation between the R and J_V follows Eq. (8). These plots exhibit a generalized relationship in a sense that they incorporate the effect of operating pressure. It can be observed from Figs. 10 and 11 that the R is also higher for the $CdSO_4$–$NiSO_4$–water system as compared to the $CdCl_2$–$NiCl_2$–water system. The difference between experimental and model results (see Fig. 11) decreases with increase in pressure. The present model does not fit properly at lower pressures in case of $CdSO_4$–$NiSO_4$–water system, which was also reported in literature [48].

5. Conclusions

In the present study, rejection experiments are performed to evaluate the ability of an NF membrane for removing cadmium and nickel ions from multicomponent aqueous solutions. At constant applied pressure of 20×10^5 N/m^2 and feed concentration of 0.005 g/L, the observed rejections of cadmium and nickel ions are found to be 80.57% and 85.27% for $CdCl_2$–$NiCl_2$–water system and 97.26% and 98.90% for $CdSO_4$–$NiSO_4$–water system, respectively. It may be concluded that this membrane has a potential for the purification of wastewater with heavy metals. In case of $CdCl_2$–$NiCl_2$–water system, the rejections of cadmium and nickel ions are strongly affected by the variation of pH. Also, the NF membrane is characterized by the Spiegler–Kedem model coupled with the film theory. The estimated membrane transport parameters and the boundary-layer thickness (in terms of D_{AB}/δ) are used to predict the performance of the membrane, in terms of ΔP and R, which showed about 14% and 20% deviation from the experimental results for $CdCl_2$–$NiCl_2$–water system and $CdSO_4$–$NiSO_4$–water system, respectively. The results show that σ and P_M depend on the type of anions of the particular salt, which is in line with the published literature.

References

[1] M.J. Gonzalez-Munoz, M.A. Rodriguez, S. Luque, J.R. Alvarez, Recovery of heavy metals from metal industry wastewaters by chemical precipitation and nanofiltration, Desalination 200 (2006) 742–744.
[2] Z. Wang, G. Liu, Z. Fan, X. Yang, J. Wang, S. Wang, Experimental study on treatment of electroplating wastewater by nanofiltration, J. Membr. Sci. 305 (2007) 185–195.
[3] H.A. Qdais, H. Moussa, Removal of heavy metals from wastewater by membrane processes: a comparative study, Desalination 164 (2004) 105–110.
[4] I. Frenzel, D.F. Stamatialis, M. Wessling, Water recycling from mixed chromic acid waste effluents by membrane technology, Sep. Purif. Technol. 49 (2006) 76–83.
[5] T.A. Kurniawan, G.Y.S. Chan, W.H. Lo, S. Babel, Physico-chemical treatment techniques for wastewater laden with heavy metals, Chem. Eng. J. 118 (2006) 83–98.
[6] N. Fiol, I. Villaescusa, M. Martinez, N. Miralles, J. Poch, J. Serarols, Sorption of Pb(II), Ni(II), Cu(II) and Cd(II) from aqueous solution by olive stone waste, Sep. Purif. Technol. 50 (2006) 132–140.
[7] S. Basha, Z.V.P. Murthy, B. Jha, Biosorption of hexavalent chromium by chemically modified seaweed, *Cystoseira indica*, Chem. Eng. J. 137 (2008) 480–488.
[8] N. Adhoum, L. Monser, N. Bellakhal, J.-E. Belgaied, Treatment of electroplating wastewater containing Cu^{2+}, Zn^{2+} and Cr(VI) by electrocoagulation, J. Hazard. Mater. 112 (2004) 207–213.
[9] J.U.K. Oubagaranadin, N. Sathyamurthy, Z.V.P. Murthy, Evaluation of Fuller's earth for the adsorption of mercury from aqueous solutions: a comparative study with activated carbon, J. Hazard. Mater. 142 (2007) 165–174.
[10] J.J. Qin, M.N. Wai, M.H. Oo, H. Lee, A pilot study for reclamation of a combined rinse from a nickel plating operation using a dual-membrane UF/RO process, Desalination 161 (2004) 155–167.
[11] N. Lamba, Z.V.P. Murthy, Raj Kumar, Membrane processing of an aqueous waste stream from catalyst manufacturing plant, Sep. Sci. Technol. 37 (2002) 191–202.

[12] L.E. Voges, M.M. Benjamin, Y. Chang, Use of iron oxides to enhance metal removal in crossflow microfiltration, J. Environ. Eng. 127 (2001) 411–419.

[13] K. Volchek, L. Keller, D. Velicogna, H. Whittaker, Selective removal of metal ions from ground water by polymeric binding and microfiltration, Desalination 89 (1993) 247–262.

[14] K. Trivunac, S. Stevanovic, Removal of heavy metal ions from water by complexation-assisted ultrafiltration, Chemosphere 64 (2006) 486–491.

[15] G. Borbely, E. Nagy, Removal of zinc and nickel ions by complexation-membrane filtration process from industrial wastewater, Desalination 240 (2009) 218–226.

[16] C.R. Tavares, M. Vieira, J.C.C. Petrus, E.C. Bortoletto, F. Ceravoll, Ultrafiltration/complexation process for metal removal from pulp and paper industry wastewater, Desalination 144 (2002) 261–265.

[17] J. Barron-Zambrano, S. Laborie, Ph. Viers, M. Rakib, G. Durand, Mercury removal from aqueous solutions by complexation—ultrafiltration, Desalination 144 (2002) 201–206.

[18] S. Petrov, V. Nenov, Removal and recovery of copper from wastewater by a complexation-ultrafiltration process, Desalination 162 (2004) 201–209.

[19] A.W. Mohammad, R. Othaman, N. Hilal, Potential use of nanofiltration membranes in treatment of industrial wastewater from Ni–P electroless plating, Desalination 168 (2004) 241–252.

[20] Y. Garba, S. Taha, N. Gondrexon, J. Cabon, G. Dorange, Mechanisms involved in cadmium salts transport through a nanofiltration membrane: characterization and distribution, J. Membr. Sci. 168 (2000) 135–141.

[21] K.H. Ahn, K.G. Song, H.Y. Cha, I.T. Yeom, Removal of ions in nickel electroplating rinse water using low-pressure nanofiltration, Desalination 122 (1999) 77–84.

[22] S. Bouranene, P. Fievet, A. Szymczyk, M.E.H. Samar, A. Vidonne, Influence of operating conditions on the rejection of cobalt and lead ions in aqueous solutions by a nanofiltration polyamide membrane, J. Membr. Sci. (2008).

[23] Z.V.P. Murthy, L.B. Chaudhari, Application of nanofiltration for the rejection of nickel from aqueous solutions and estimation of membrane transport parameters, J. Hazard. Mater. 160 (2008) 70–77.

[24] A.G. Boricha, Z.V.P. Murthy, Preparation, characterization and performance of nanofiltration membranes for the treatment of electroplating industry effluent, Sep. Purif. Technol. 65 (2009) 282–289.

[25] Z.V.P. Murthy, L.B. Chaudhari, Separation of binary heavy metals from aqueous solutions by nanofiltration and characterization of the membrane using Spiegler–Kedem model, Chem. Eng. J. 150 (2008) 181–187.

[26] L.S. Clesceri, A.E. Greenberg, A.D. Eaton, Standard Methods for the Examination of Water and Wastewater, 20th ed., American Public Health Association, American Water Works Association, and Water Environment Federation, Washington, DC, 1998.

[27] V.K. Gupta, S.T. Hwang, W.B. Krantz, A.R. Greenberg, Characterization of nanofiltration and reverse osmosis membrane performance for aqueous salt solutions using irreversible thermodynamics, Desalination 208 (2007) 1–18.

[28] V. Gekas, B. Hallstrom, Mass-transfer in the membrane concentration polarization layer under turbulent cross flow. 1. Critical literature—review and application of existing Sherwood correlations to membrane operations, J. Membr. Sci. 30 (1987) 153–170.

[29] Z.V.P. Murthy, S.K. Gupta, Estimation of mass transfer coefficient using a combined nonlinear membrane transport and film theory model, Desalination 109 (1997) 39–49.

[30] K.S. Spiegler, O. Kedem, Thermodynamics of hyperfiltration (reverse osmosis): criteria for efficient membranes, Desalination 1 (1966) 311–326.

[31] G.T. Ballet, L. Gzara, A. Hafiane, M. Dhahbi, Transport coefficients and cadmium salt rejection in nanofiltration membrane, Desalination 167 (2004) 369–376.

[32] K. Mehiguene, Y. Garba, S. Taha, N. Gondrexon, G. Dorange, Influence of operating conditions on the retention of copper and cadmium in aqueous solutions by nanofiltration: experimental results and modeling, Sep. Purif. Technol. 15 (1999) 181–187.

[33] S. Koter, Determination of the parameters of the Spiegler–Kedem–Katchalsky model for nanofiltration of single electrolyte solutions, Desalination 198 (2006) 335–345.

[34] M. Soltanieh, W.N. Gill, Review of reverse osmosis membranes and transport models, Chem. Eng. Commun. 12 (1981) 279–363.

[35] A.L. Ahmad, M.F. Chong, S. Bhatia, Mathematical modeling of multiple solutes system for reverse osmosis process in palm oil mill effluent (POEM) treatment, Chem. Eng. J. 132 (2007) 183–193.

[36] Z.V.P. Murthy, S.K. Gupta, Sodium cyanide separation and parameters estimation for reverse osmosis thin film composite polyamide membrane, J. Membr. Sci. 154 (1999) 89–103.

[37] Z.V.P. Murthy, S.K. Gupta, Thin film composite polyamide membrane parameters estimation for the phenol–water system by reverse osmosis, Sep. Sci. Technol. 33 (1998) 2541–2557.

[38] C. Bhattacharjee, P.K. Bhattacharya, Ultrafiltration of black liquor using rotating disk membrane module, Sep. Purif. Technol. 49 (2006) 281–290.

[39] A. Apelblat, E. Korin, The vapour pressures over saturated aqueous solutions of cadmium chloride, cadmium bromide, cadmium iodide, cadmium nitrate, and cadmium sulphate, J. Chem. Thermodyn. 39 (2007) 1065–1070.

[40] M.E.L. Guendouzi, A. Mounir, A. Dinane, Water activity, osmotic and activity coefficients of aqueous solutions of Li_2SO_4, Na_2SO_4, K_2SO_4, $(NH_4)_2SO_4$, $MgSO_4$, $MnSO_4$, $NiSO_4$, $CuSO_4$, and $ZnSO_4$ at T = 298.15 K, J. Chem. Thermodyn. 35 (2003) 209–220.

[41] C. Venkateswarlu, J. Ananthaswamy, Thermodynamics of electrolyte solutions: activity coefficients of NaCl in the NaCl–$NiC1_2$–H_2O system at 25, 35, and 45 °C, Can. J. Chem. 68 (1990) 294–297.

[42] J.M.M. Peeters, J.P. Boom, M.H.V. Mulder, H. Strathmann, Retention measurements of nanofiltration membranes with electrolyte solutions, J. Membr. Sci. 145 (1998) 199–209.

[43] Y. Garba, S. Taha, J. Cabon, G. Dorange, Modeling of cadmium salts rejection through a nanofiltration membrane: relationships between solute concentration and transport parameters, J. Membr. Sci. 211 (2003) 51–58.

[44] P. Vanysek, Ionic conductivity and diffusion at infinite dilution, in: D.R. Lide (Ed.), CRC Handbook of Chemistry and Physics, 84th ed., CRC Press, Boca Raton, FL, 2005.

[45] J. Schaep, B. Van der Bruggen, C. Vandecasteele, D. Wilms, Influence of ion size and charge in nanofiltration, Sep. Purif. Technol. 14 (1998) 155–162.

[46] N. Frares, S. Taha, D. Dorange, Influence of the operating conditions on the elimination of zinc ions by nanofiltration, Desalination 185 (2005) 245–253.

[47] M.S. Bazaraa, H.D. Sherali, C.M. Shetty, Nonlinear Programming Theory and Applications, 2nd ed., John Wiley & Sons, NJ, 1993.

[48] S.Y. Vaidya, A.V. Simaria, Z.V.P. Murthy, Reverse osmosis transport models evaluation: a new approach, Indian J. Chem. Technol. 8 (2001) 335–343.